Journal of Thermal Analysis, Vol. 47 (1996) 1463-1483

TEMPERATURE- AND HYDRATION-DEPENDENCE OF MOLECULAR MOBILITY IN SEEDS

P. Pissis[1], *A. A. Konsta*[1], *S. Ratković*[2,3], *S. Todorović*[2] *and J. Laudat*[4]

[1]National Technical University of Athens, Department of Physics, 157 80 Athens, Greece
[2]Center for Multidisciplinary Studies, University of Belgrade, Belgrade, Yugoslavia
[3]Maize Research Institute 'Zemun Polje', 11080 Zemun-Belgrade, Yugoslavia
[4]Charles University, Institute of Physics, Ke Karlovu 5, 12116 Prague 2, Czech Republic

Abstract

Broad-band ac dielectric relaxation spectroscopy (DRS) and various techniques of thermally stimulated currents (TSC) have been used to investigate molecular mobility in cereal and legume seeds, over wide ranges of water content and temperature. We focused our interest on the detailed study of the interactions between water and seed constituents. The results are quantitatively discussed, using various concepts dictated by the experimental techniques employed and in relation to the protein and carbohydrate contents of the seeds. In addition, the glass transition in the seeds, freezing and melting of water, and the protonic conduction process have been studied in some detail.

Keywords: dielectric relaxation spectroscopy, glass transition, protonic conductivity, seed hydration, thermally stimulated currents

Introduction

The hydration properties of seeds have been studied by means of various experimental techniques, including water sorption isotherms and water imbibition measurements [1–3], differential scanning calorimetry (DSC) and specific-heat measurements [4, 5], diffusion measurements [6], nuclear magnetic resonance (NMR) [6, 7], mechanical measurements [8–10], spin-probe electron paramagnetic resonance (EPR) [11–13], thermally stimulated depolarization currents (TSDC) measurements [12–14], dc conductivity calculations from dielectric measurements [2, 15, 16], and dielectric relaxation spectroscopy (DRS) [17–24].

Modifications of structural and dynamic characteristics of water in seeds, compared to the corresponding characteristics of bulk water, resulting from interactions of water molecules with seed constituents, have been a popular topic of investigation [1–3, 5–8, 11, 14, 17, 18]. Depending on the investigator's approach and the experimental method used, water in seeds has often been classi-

0368–4466/96/ $ 5.00

John Wiley & Sons, Limited
Chichester

fied into different types, such as molecularly distributed and clustered water, free (bulk) and bound water, or freezable and nonfreezable water. In this context, we remind the reader of the old but still very useful review by Kuntz and Kauzmann [25] on the interaction of water with proteins, one of the main constituents of seeds, and draw the reader's attention to a more recent one on the same subject by Rupley and Carreri [26].

Molecular mobility in seeds has been found to be substantially influenced by water. In this respect, two topics have been studied in some detail. The first involves the glass transition in seeds and the dependence of the glass transition temperature (T_g) on water content [2, 4, 5, 9, 10, 12–14]. The second topic involves electrical dc conductivity in hydrated seeds. Carreri and coworkers interpreted the results of their dielectric ac measurements on hydrated seeds in terms of percolative proton transfer along threads of hydrogen-bonded water molecules on the macromolecular surface [2, 15, 16]. The relationship of the physical effects of glass transition and percolation to biological effects (germination of seeds) has also been investigated in the context of efforts to describe and understand biological functions in physical terms [2, 12, 13]. The glass transition in proteins and foods, in relation to water content, has been the subject of two recent reviews [27, 28].

Investigation of the dependence of physical properties of a seed/water system on water content forms the basis for developing methods for non-destructive measurements of water content in seeds. Dielectric measurements have been considered to be well suited to this aim [1, 4, 20–24]. In a series of papers, Nelson and coworkers developed the principles of simultaneous, on-line determination of moisture content and density of seeds and other agricultural products by radio-frequency and microwave measurement techniques [20–24].

It follows, from a thorough study of the literature on hydration properties of seeds, that more work is needed to better understand various aspects of the topics involved. A major problem is that the various concepts used to describe the interactions of water with seed constituents depend on, and/or are dictated by, the particular technique used [29]. We should always take that into account when comparing hydration results obtained by different techniques. In their review [27], Levine and Slade criticised, as potentially misleading, the use of concepts that divide hydration water into different classes, such as free and bound or freezable and non-freezable, and argued for a 'food polymer science' approach, which unifies structural aspects of foods with functional aspects, dependent on mobility, and described in terms of the integrated concepts of 'water dynamics' and 'glass dynamics'. Even if we consider only techniques that measure molecular mobility, e.g. in the glass transition region, we should bear in mind that not only the time scales (frequencies) of the techniques used (and of formalisms used to present the data obtained by the same technique, e.g. compliance and modulus [30]) may be different, but also that the space (local) scale is, in general, different for different techniques. The latter is due to the

fact that various techniques, such as DSC, NMR, EPR, DMA (dynamic mechanical analysis), and DRS, probe the mobility of molecular units of different sizes [27, 30, 31].

In this paper, we report results of our investigations of hydration properties of various ground seeds, determined by means of broad-band DRS in the frequency range 5 Hz–2 GHz and temperature range 170–320 K, and of various techniques of thermally stimulated currents (TSC) in the temperature range 85–300 K. The TSC techniques included TSDC, thermally stimulated polarization currents (TSPC), and dc-conductivity. Cereal and legume seeds of different genotypes (wheat, triticale, maize, bean, horsebean, chick pea, white lupine, african pea) having different chemical compositions (proteins, carbohydrates, lipids), were analyzed. Preliminary DRS and TSDC measurements, made for all these genotypes at different water contents, show that from the dielectric point of view, cereals behave differently than legumes, in agreement with NMR results [7]. As a consequence, results reported here concern mainly bean and wheat seeds, which have been studied in more detail, as well as triticale, of which different parts have been sudied (endosperm, perisperm and pericarp).

The water content, h, defined as grams of water/gram of dry material, was systematically varied between 0 and 0.50. Please note that this is the h range relevant to physiological activity in seeds [5, 28]. At ambient temperature and relative humidity, the physiological water contents of the seeds investigated were 0.11–0.13. Progressive lowering of h below this range results in accelerated deterioration of the seeds. Metabolism becomes increasingly facilitated in the h range 0.24–0.35, whereas germination requires h values higher than about 0.6 [5]. In TSC measurements on one type of cereal (triticale), h was varied up to 6.0.

The following aspects of hydration are stressed in discussing our experimental results:

(1) the interactions between water and seed constituents, resulting in modifications of their dynamic characteristics. In this respect, it is interesting to compare cereals and legumes: in general, cereals contain less protein and more carbohydrate than do legumes [7]. Depending on the experimental technique and conditions used, results are discussed in terms of free and bound water, freezable and non-freezable water, plasticization of local chain motions, molecularly distributed water, clustered and microphase-separated water. Results obtained for the same sample with different techniques are critically compared, and the relationships among the different descriptions, dictated by the various techniques, are discussed in a quantitative way.

(2) the glass transition in seeds, and melting and freezing events of water. Often, glass transition signals in hydrated systems at high water contents are masked by freezing and melting events of water in DSC measurements, and by high values of conductivity in DRS measurements [32]. In such cases, TSC techniques are well suited for measuring T_g and glass transition dynamics [33].

(3) the dependence of the directly measured, thermally stimulated dc conductivity on water content h, in terms of percolation [2 ,15, 16].

(4) the question of whether dielectric measurements at frequencies lower than radio or microwave, and in a broad frequency range rather than at a fixed frequency [20, 24], may be suitable for non-destructive monitoring of water content in seeds. This question may have practical implications, in view of the new generation of completely automatic Frequency Response Analyzers, Impedance Analyzers, and Network Analyzers, capable of covering broad frequency ranges within a few minutes or even seconds. We might learn here from parallel developments in using DRS for monitoring chemical reactions, such as curing of polymers [34].

Experimental

Materials

For the preparation of samples for DRS and TSC measurements, seeds were uniformly ground, and the powder was compressed, at 6 tons, into cylindrical pellets of 13 mm diameter and 1.5–2.0 mm thickness. The densities of dry pellets of the various seeds were between 1.10 and 1.20 g cm^{-3}. h was varied up to about 0.5, by equilibrating the samples in closed jars over saturated salt solutions of known relative humidities. The value of h was determined by weighing. Vacuum-drying at 383 K and 5×10^{-2} torr for 24 h was adopted for the determination of dry weights.

For one of the seed genotypes (triticale), three different samples were investigated by TSC: prepared from ground whole seed, from endosperm (flour), and from pericarp with embryo and perisperm (pigmeal). For these triticale samples, the water content was varied up to 6.0 by mixing the powder with doubly distilled, deionized water (16 MΩ cm^{-1}).

Dielectric relaxation spectroscopy (DRS)

DRS is a powerful technique, widely used for investigations on molecular mobility in a variety of materials [34, 35]. The main advantage of DRS, compared to other spectroscopic techniques, is its extremely wide range of frequencies, from as low as 10^{-4} Hz to as high as 10^{11} Hz, which can be covered by combining several experimental arrangements. This remarkable breadth enables one to relate the observed dielectric response to a specific polarization mechanism. The contribution to overall polarization comes from the moieties or particles whose relaxation times are faster than the applied signal, which enables one to distinguish different processes by their different frequency dependencies. There are various contributions to dielectric polarization and re-

laxation of hydrated biomaterials in the above frequency range. In the order of increasing frequency, and roughly schematizing, they arise from electrode polarization, free charge migration, Maxwell-Wagner-Sillars or interfacial polarization in heterogeneous systems, and dipole orientation [24, 35]. The relaxation of atomic and electronic charges occurs at still higher frequencies than those employed in dielectric measurements [34].

Experimental dielectric data are customarily presented in terms of the complex permittivity, defined as

$$\varepsilon^* = \varepsilon' - i\varepsilon'' \tag{1}$$

The real, ε', and imaginary, ε'', components of the dielectric permittivity are related to the capacitance, C, and the conductance, S, of the sample measured during the experiment, by:

$$\varepsilon' = \frac{Cd}{A\varepsilon_o} = \frac{C}{C_o} \tag{2}$$

$$\varepsilon'' = \frac{G}{\omega\varepsilon_o} = \frac{S}{\omega C_o} \tag{3}$$

In these equations, A is the electrode area, d the spacing between electrodes, ε_o the permittivity of free space, G the conductivity, ω the angular frequency of the applied field ($\omega = 2\pi f$, f the applied frequency), and C_o the equivalent capacitance of free space, $C_o = A\varepsilon_o/d$ [34, 35].

Two different experimental arrangements, both completely automatic, were used for DRS measurements: a Hewlett Packard HP 4292A Impedance Analyzer, combined with an Ando-type TO-19 thermostatic oven and Ando SE-70 dielectric cell; and Hewlett Packard HP 3577B and HP 8510B Network Analyzers, combined with a home-made cryostat and dielectric cell. The frequency and temperature ranges covered were 5 Hz – 2 GHz and 170–320 K, respectively. The experimental data were analyzed using various formalisms, to extract as much information as possible: complex permittivity, ac conductivity, complex impedance, and electric modulus [35].

TSC techniques

The TSDC technique consists of measuring the thermally activated release of stored electric polarization, as follows [37]. A sample is polarized by an applied electric field, E_P, at a temperature, T_P, for a time, t_P. This polarization is subsequently frozen-in by cooling the sample to a temperature, T_o, sufficiently low to prevent depolarization by thermal energy. The electric field is then

switched off, and the sample is warmed at a constant rate, b(b =3–5 K min^{-1} in our experiments), while the depolarization current is detected by an electrometer.

In the case of a single dipolar relaxation process that obeys the Arrhenius equation: $\tau(T)=\tau_o \exp(W/kT)$, the depolarization current density, $J(T)$, is given by

$$J(T) = \frac{P_o}{\tau_o} \exp\left(\frac{-W}{kT}\right) \exp\left(-\frac{1}{b\tau_o}\int_{T_o}^{T} \exp\left(\frac{-W}{kT}\right) dT'\right) \quad (4)$$

where τ is the relaxation time, W the activation energy of the relaxation, τ_o the pre-exponential factor, T the absolute temperature, k Boltzmann's constant, and P_o the initial polarization. Analysis of the shape of the peak represented by Eq. (4) makes it possible to obtain the activation energy, the pre-exponential factor, and the contribution, $\Delta\varepsilon$, of the peak to the static permittivity. In order to investigate the multiplicity of the peaks, the techniques of partial heating and thermal sampling [37] have been applied. In the thermal sampling technique, the sample was continuously cooled at a constant rate, and the polarizing electric field was switched on at T_p and switched off at a slightly lower temperature, T_d, i.e. the relaxation processes within a narrow temperature range were sampled. The temperature window (T_p–T_d) used was 3 K. In the partial heating technique, the sample was polarized in the usual way and then partially depolarized by partial heatings, separated by rapid coolings, up to a series of cut-off temperatures that span the whole temperature range of the peak.

In TSPC measurements, the depolarized sample is cooled to low temperatures. The electric field is then switched on, and the sample is warmed at a constant rate. The recorded TSPC spectra typically consist of contributions from both relaxation effects at lower temperatures and dc conductivity at higher temperatures. The method allows one to observe dipole ordering, determine the temperature range where ohmic conductivity dominates, and determine the conditions of optimal T_p [37].

In dc conductivity measurements, a dc electric field (typically 10^5 V m^{-1}) is applied during both cooling and heating.

Two different experimental arrangements, described in detail elsewhere [38, 39], were employed for TSC measurements.

Experimental errors

Typical experimental errors were as follows. In measurements of water content, h, ±0.01; in TSC measurements: ±2 K for the temperature of maximum current (peak temperature), T_m; ±0.02 eV for the activation energy, W; and a factor of about two in τ_o. In DRS measurements, the temperature is stabilised to better than ±0.2 K, and the errors in ε' and ε'' are ±5. These errors refer to

measurements on the same sample, whereas, for measurements on different samples from the same genotype at the same water content, the errors are larger by about a factor of two.

Results and discussion

DRS

Figure 1 shows log-log plots of the real and imaginary parts of the dielectric permittivity, ε' and ε'', respectively, and of the ac conductivity, G, *vs.* frequency, f, for wheat at $h=0.12$ and temperatures between 193 and 273 K. The h value of 0.12 corresponds to the sample's water content at ambient temperature (293 K) and relative humidity (60%). A dispersion, i.e. a step in the ε' plot, and maxima in the ε'' and tan$D$ (tan$D=\varepsilon''/\varepsilon'$, not shown here) plots, is clearly observed; it shifts to higher frequencies with increasing temperature, from about 10^3 Hz at 193 K to about 10^8 Hz at 293 K. In Fig. 2, we show the corresponding Arrhenius plots, i.e. $\ln f_m$ *vs.* $1/T$, where f_m is the frequency of maximum ε'' and tan$D$, respectively, for that dispersion. The frequency position of the dispersion and the range of W values suggest that the dispersion is due to the motion of short side-chains of proteins and carbohydrates [40]. At frequencies lower than those of the step in the ε' plot and of the peak in the ε'' and tan$D$ plots, the side-chains can follow the changes of the applied ac electric field and thus contribute by their polarization to ε', whereas at higher frequencies, they can no longer follow the changes of the ac field. Support for this interpretation will come from TSDC measurements reported in the next section. The dispersion shows the effect of plasticization by water, i.e. it shifts to higher frequencies with increasing water content at constant temperature. Data for this plasticizing action of water, which is very similar to the plasticizing effect of temperature shown in Fig. 1, are obtained by TSC techniques and will be shown in Fig. 6. The dispersion is characterized by broad half width values, a typical feature of local side-chain relaxations in polymers and biopolymers [41]. The frequency position, shape, and water-content dependence of this dispersion are practically independent of seed genotype. However, this may simply be due to the broadness of the dispersion and the difficulties in unequivocally deconvoluting it into individual contributions, which might be characteristic of seed genotype. We will come back to this problem in the next section.

The spectra in Fig. 1 become more complex at frequencies lower than those of the dispersion described above. It is believed that main-chain relaxations, space-charge effects, and charge-carrier motions, giving rise to conductivity, may contribute to the spectra at low frequencies, depending on temperature and water content. TSC measurements, which are characterized by higher resolving power (reported in the next section), help to resolve the different contributions.

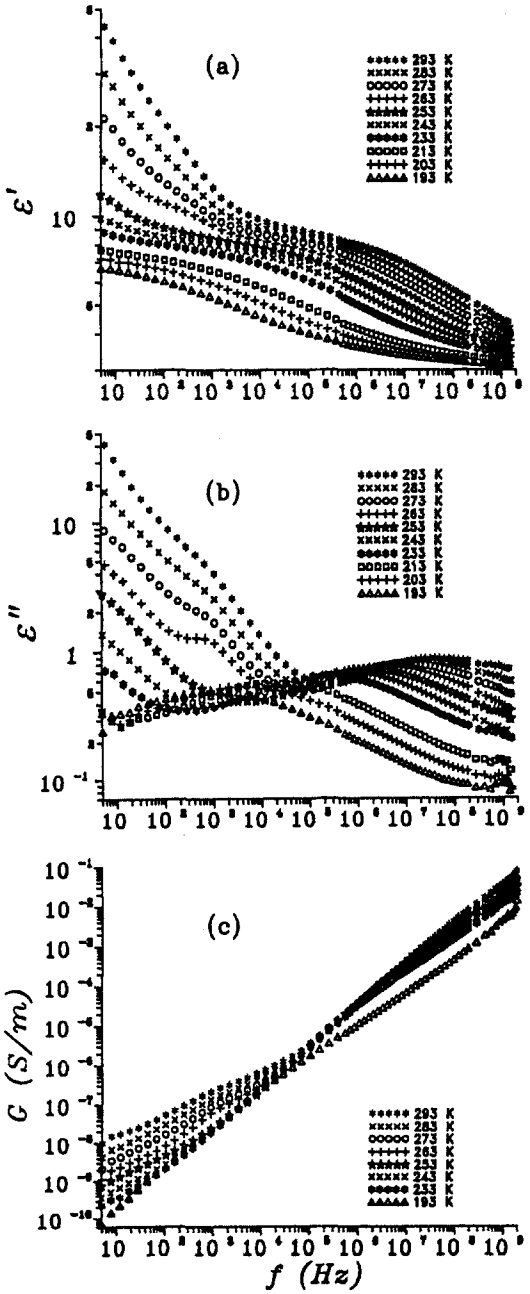

Fig. 1 Log-log plots of a) the real, ε′, and b) the imaginary, ε″ , part of the complex permittivity, and c) ac conductivity, G, *vs.* frequency, f, for wheat at $h=0.12$ and various temperatures

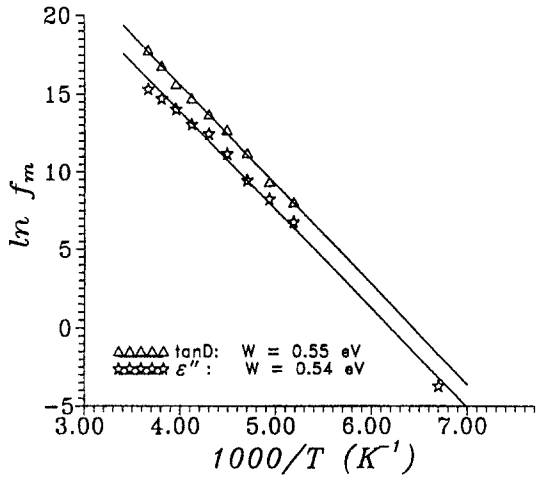

Fig. 2 Arrhenius plots, i.e. lnf_m, *vs.* $1/T$, where f_m is the frequency (in Hz) corresponding to the maxima of ε'' and tan D, for a wheat flour sample with $h=0.12$, evaluated from the spectra of Fig. 1b. The last point on the right corresponds to the low temperature peak of the TSDC plot, recorded for an identical sample

However, some points here deserve further comment. The high values of ε' at low frequencies, which become as high as 10^6 at high temperatures and water contents, and which are obviously not bulk values, indicate the existence of so-called space-charge polarization [42]. On the other hand, the apparent dielectric loss also becomes very high at low frequencies and high water contents, due to free-charge motion within the sample, referred to as conductivity relaxation [35]. Presentation of the same experimental data in the modulus formalism [43], i.e. plots of M' (f) and M'' (f), where M' and M'' are, respectively,the real and imaginary parts of the complex modulus, M^*

$$M^* = 1/\varepsilon^* \tag{5}$$

$$M' = \frac{\varepsilon'}{\varepsilon'^2 + \varepsilon''^2} \tag{6}$$

$$M'' = \frac{\varepsilon''}{\varepsilon'^2 + \varepsilon''^2} \tag{7}$$

reveal a new dispersion at low frequencies. In fact, Fig. 3 shows, in a semilog plot, $M''(f)$ for a bean flour sample with $h=0.13$. The dispersion observed at high frequencies has the same origin as that of the ε'' dispersion shown in Fig. 1, i.e. local motion of short side-chains of proteins and carbohydrates. In the different formalisms, a shift of the dispersion to higher frequencies is observed in

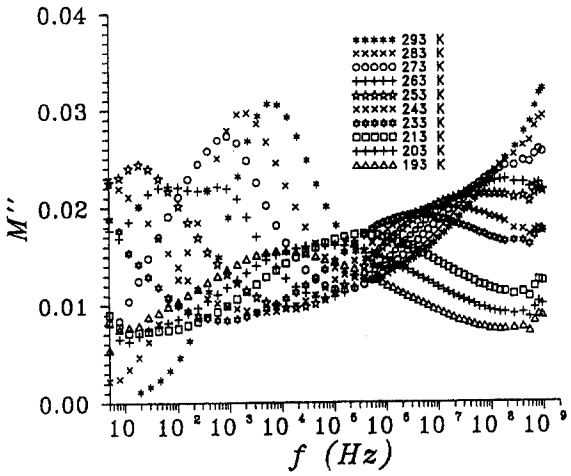

Fig. 3 Plot of the imaginary part of the modulus, M'', *vs.* frequency, f, for a bean sample at $h=0.12$ and various temperatures

the order ε'', tan$D$, and M'', in agreement with theory [35, 43]. The new dispersion at low frequencies also shifts to higher frequencies with increasing T. It corresponds to the contribution of conductivity in the ε'' plots of Fig. 1. The activation energy of this dispersion, $W=0.60$–0.70 eV, is, within the limits of experimental error, the same as that for dc conductivity, as measured on identical samples (see next section). This is a strong indication that conductivity relaxation contributes to the spectra at low frequencies and gives rise to the observed low frequency peak in $M''(f)$ [35, 43].

It is interesting to note here that an additional dispersion is observed at $T>263$ K in the frequency region around 10^3 Hz. This dispersion gives rise to a peak or shoulder in the $\varepsilon''(f)$ plots of Fig. 1 and is also observed in the $M''(f)$ plots (Fig. 3). We have no explanation at his stage for this dispersion.

Figures 4 and 5 show, in log-log presentation, the ac conductivity spectra of wheat, for $h=0.22$ and several temperatures and for 273 K and several water contents, respectively. Similarly to the results shown in Fig. 1c, the ac conductivity increases at low frequencies with increasing temperature and water content. It is interesting to note in Fig. 4 that there are no discontinuous changes of ac conductivity with temperature decreasing to 203 K. Such discontinuous changes at subzero temperatures have been observed for water contents higher than about 0.30, and are attributed to freezing of pure water in a separate phase. At these critical subzero temperatures, the conductivity behaviour changes abruptly from typical conductor-like to typical insulator-like. As an example, we show in Fig. 6 ac conductivity data for a wheat sample at $h=0.42$ and several temperatures. These data are to be compared with those shown in Fig. 4. We observe in Fig. 6, for temperatures higher than 263 K, high values of conductivity, which are only slightly frequency-dependent. This is the typical be-

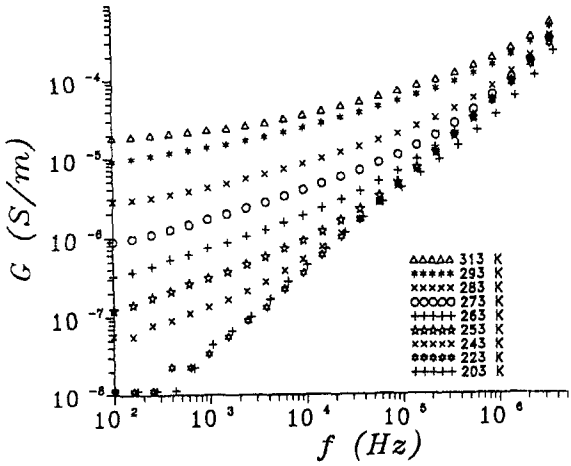

Fig. 4 Log-log plots of ac conductivity, G, *vs.* frequency, f, for wheat at $h=0.22$ and various temperatures

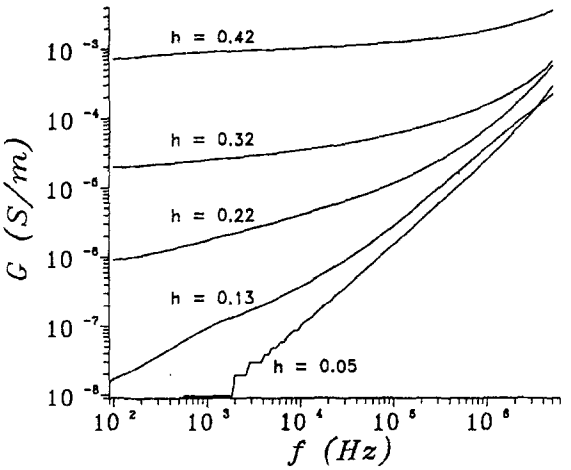

Fig. 5 Log-log plots of ac conductivity, G, *vs.* frequency, f, for wheat at 273 K and several water contents

haviour of a conductor, and the conductivity values are those of dc conductivity. At high conductivity values (high T), electrode polarization is observed as a drop in conductivity at low frequencies [35]. The conductor-like behaviour of the sample in Fig. 6 at 263 K, and the high value of dc conductivity, suggest ion conduction through a separate water phase [35]. At $T<263$ K, in Fig. 6, conductivity decreases and shows strong frequency-dependence. This behaviour, typical for an insulator, suggests freezing of the separate water phase. System-

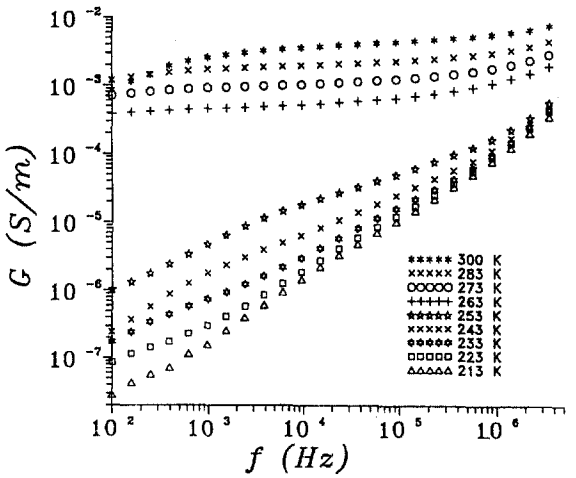

Fig. 6 Log-log plots of ac conductivity, G, *vs.* frequency, f, for wheat at $h=0.42$ and various temperatures, showing the effect of ice crystallization at $T<223$ K

atic investigations at several water contents showed that the temperature of discontinuous changes in ac conductivity, interpreted as a freezing temperature in cooling scans and as a melting temperature in heating scans, increases toward 273 K with increasing h and shows hysteresis. These results suggest that the water content of about 0.30 represents a distinct hydration level, in the sense that the seed/water system is a homogeneous one at $h \leq 0.30$ and a heterogeneous one at $h > 0.30$. In other words, at $h > 0.30$, a separate phase exists, which crystallises at low temperatures, whereas at $h \leq 0.30$, water is distributed molecularly and/or in small clusters, so that no crystalline ice is formed even at very low temperatures. Please note here that the terms homogeneous and heterogeneous refer only to the distribution of water in the ground seed sample, which is itself heterogeneous at the molecular level. The above findings are in good agreement with results of calorimetric studies of water in seed tissues [5].

The increase of ac conductivity with h in Fig. 5 is indicative of the plasticizing action of water. At $h > 0.30$, conduction of ions, which are likely to be protons, occurs through the separate water phase, and the conductivity behaviour of the sample changes from insulator-like at low h values to conductor-like at higher h values. The results in Fig. 5 suggest that measurements of ac conductivity at lower frequencies might be used to monitor the water content of seeds, as an interesting alternative to measurements at radio- and MW-frequencies [20–24]. We note in this respect that the data in Fig. 5 at each water content are sampled within a few seconds, and that for monitoring water content, there is no need, in principle, to perform the measurements at a fixed frequency.

We note the similarity of Figs 4 and 5. An increase in temperature (T) at constant water content (h) causes the same effect as an increase in h at constant T.

This finding is a manifestation of the *T-f-h*-superposition principle, which states that the plasticizing effect of increasing h at constant T is equivalent to the effect of increasing T at constant h, both effects leading to an enhancement of molecular and charge mobility [27, 44].

It is interesting to compare wheat and bean samples with respect to their conductivity behaviour. At water contents higher than about 0.30, conductivity is dominated by the presence of a separate water phase, irrespective of the nature of the matrix. Approximate values of dc conductivity can be obtained in this h-range from the plateaus of ac conductivity spectra (Figs 5 and 6). Extrapolation to zero frequency may lead to significant errors because of electrode effects [42], an example of which is shown in Fig. 5 for $h=0.42$, and in Fig. 6 for $T>273$ K. At lower h values, bean and wheat samples behave differently; bean samples exhibiting, at the same temperature and water content, higher values of conductivity (by 1–2 orders of magnitude) and more conductor-like behaviour. We suggest that this difference is related to the higher protein content of beans, in comparison to wheat [7].

TSC techniques

Figure 7 shows TSDC, TSPC and dc conductivity thermograms, measured on triticale samples at $h=1.92$ and 0.10. The TSDC curves exhibit two complex relaxation bands. The low-temperature (LT) band in the range of 80–150 K con-

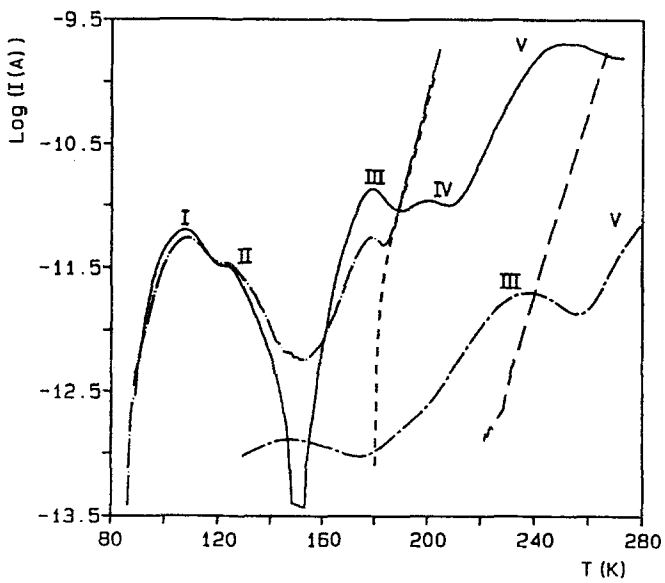

Fig. 7 TSDC, TSPC and dc conductivity *vs.* frequency, f, for a triticale sample at two different water contents, h. TSDC at $h=1.92$ (–), TSPC at $h=1.92$ (– · –), dc conductivity at $h=1.92$ (---), TSDC at $h=0.10$ (– - –), and dc conductivity at $h=0.10$ (– –)

sists of as many as two overlapping peaks, numbered I and II in the order of increasing temperature. The high-temperature (HT) band in the range of 150–300 K consists of as many as three overlapping peaks, numbered III–V in the order of increasing temperature. The number of peaks in each band, their temperature positions, and their magnitudes change with water content (Fig. 8). TSDC curves similar to those in Figs 7 and 8 were also obtained for endosperm, pericarp and perisperm samples from triticale.

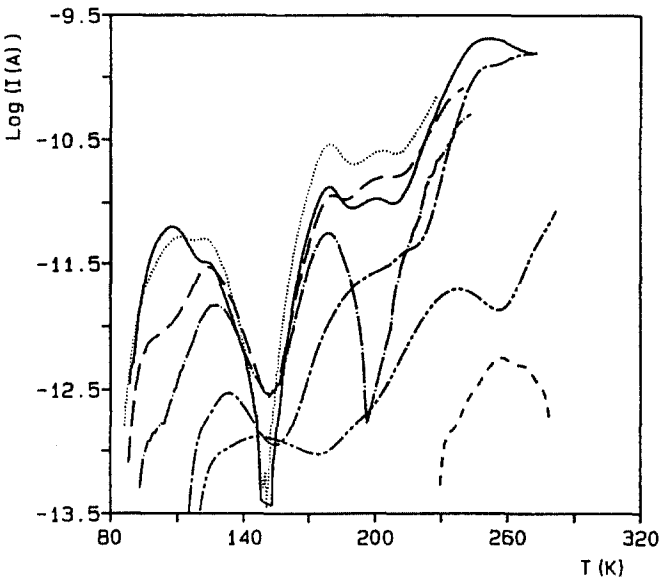

Fig. 8 TSDC spectra for a triticale sample at several water contents: $h=1.92$ (–), 0.88 (...), 0.58 (---), 0.36 (– · –), 0.16 (- – -), 0.10 (– -- –) and 0.07 (– – –)

The LT band, apparent at even higher temperatures (170–180 K) even for very low water contents ($h=0.01$), shifts to lower temperatures and increases in magnitude with increasing water content (Figs 9 and 10). This band is attributed to reorientation of short side-chains of the seed-constituent proteins and carbohydrates, due to plasticization by water. This interpretation is strongly supported by results of TSDC measurements on proteins and carbohydrates [45, 46]. Thus, the origin of the LT TSDC band is similar to that of the dispersion in Fig. 1. This is verified by extrapolation of the $\ln f_m$ *vs.* $1/T$ straight line in the Arrhenius plot of Fig. 2 to 143 K, the peak temperature of the LT band measured for a bean sample at $h=0.12$, and assuming an equivalent frequency of 2.5×10^{-2} Hz for TSDC measurements [37]. Thermal-sampling and partial-heating techniques were used to measure the spectra of activation energies [45, 46] in the LT band. The values of W determined in this way are typically lower than those from ac measurements shown in Fig. 2. The relationship be-

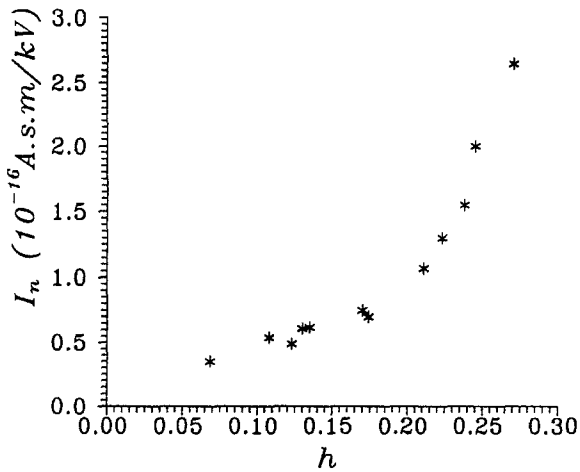

Fig. 9 Dependence of the normalized current maximum, I_n, of the low-temperature TSDC band on water content, h, for bean

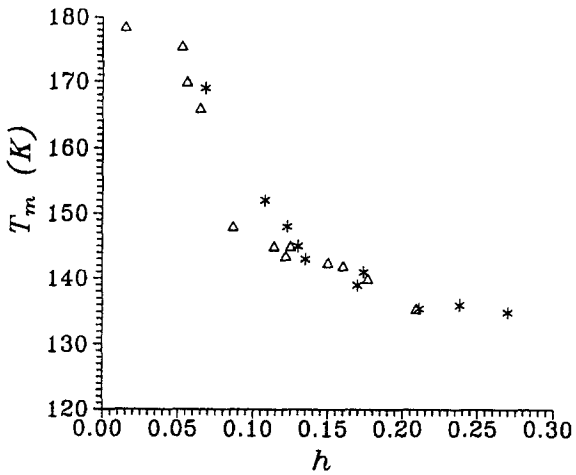

Fig. 10 Dependence of the peak temperature, T_m, of the low-temperature TSDC band on water content, h, for bean (*) and wheat (Δ) flours

tween W values from ac and TSDC measurements in different temperature regions and possible compensation by τ_o, are still open questions [35]. Thermal-sampling and partial-heating measurements on samples of different genotypes at the same water content are now in progress, which are aimed at investigating the question of whether individual contributions to the LT band (and to the dispersion in Fig. 1) might be characteristic of seed genotype.

At higher water contents, a new contribution to the LT band, located at about 135 K, appears (peak II in Fig. 8). This contribution results in a change in the

rate of increase of the normalized current maximum, I_n, of the LT band in Fig. 9, at about $h=0.17$, which cannot be explained solely by plasticization. I_n is normalized to constant surface area, polarizing field and heating rate, and it is a measure of the number of relaxing units contributing to the band [39]. The results in Fig. 9 are in agreement with those in Fig. 10, where it is observed that, for bean, the peak temperature, T_m, of the LT band becomes practically independent of h for $h \geq 0.17$, whereas, for wheat samples, T_m becomes practically independent of h at significantly lower values ($h \geq 0.11$), as shown on the same figure (Fig. 10).

Based on an interpretation of similar results obtained for proteins, carbohydrates and other biological materials [39, 45, 46], we attribute the additional contribution at about 135 K to the relaxation of loosely bound water molecules. Thus, water, up to about $h=0.17$ and 0.11 for bean and wheat respectively, is tightly (irrotationally) bound to primary hydration sites. The higher h value for bean than for wheat can be attributed to the higher protein content of bean, as suggested by NMR and water-imbibition measurements [7].

In Figs 7 and 8, peak I, located at about 105 K, appears on the low-temperature side of peak II, for water contents higher than about 0.50, and increases in magnitude with increasing h. It becomes larger than peak II for $h \geq 0.90$ (Fig. 8). The magnitude of the LT band increases linearly with increasing polarizing field, E_p, indicating that peaks I and II are of dipolar origin [37]. The temperature position of peak I, its mean activation energy of $W=0.28\pm0.04$ eV (obtained from thermal sampling and partial-heating measurements), and the dependence of its magnitude on h indicate that the peak is due to relaxation of free (bulk) water, which forms a separate phase and freezes at low temperatures [39]. Thus, two critical hydration levels are determined from these detailed studies of the LT TSDC band: $h=0.17$ and $h=0.11$ in bean and wheat, respectively, for the fraction of tightly bound water at primary hydration sites; and $h \approx 0.50$ in triticale for the appearance of free (bulk) water. These values compare quite well with critical hydration levels previously determined by DSC [5].

Similar to the LT band, peak III in the HT band appears in both TSDC and TSPC measurements (Fig. 7). Dc conductivity has its onset in the temperature region of peak III and then increases very sharply with increasing temperature, especially at high water contents. Consequently, TSPC is dominated by dc conductivity for temperatures higher than those of peak III, so that peaks IV and V are not observed in the TSPC curves (Fig. 7).

Figure 11 shows the dependence of peak temperature, T_M, of peak III on h for powders from triticale seeds, endosperm and perisperm and pericarp. T_M decreases sharply with increasing h and levels off at about 180 K for $h \geq 0.4$–0.5. The plot in Fig. 11, the dipolar character of peak III, the onset of dc conductivity in its temperature region [47], and similar results obtained for proteins and other biological systems [39, 47, 48] all suggest that peak III is

associated with a glass transition of the seed matrix-bound water system [2, 4, 5, 9, 10, 12–14]. Accordingly, T_M of peak III may be considered as the glass transition temperature, T_g, in agreement with results of combined studies of synthetic polymers and hydrogels by TSDC and DSC [31–33]. Thus, T_g is situated around room temperature in dry seeds and shifts sharply, with increasing h, down to temperatures around 180 K for fully hydrated seeds, due to plasticization by water. The biological implications of similar findings have been previously discussed in detail elsewhere [13, 14, 26–28].

Peak IV is located in the temperature region associated with an apparent dc conductivity of the samples. It decreases in magnitude and shifts to higher temperatures with decreasing h (Fig. 8). Its activation energy is about 0.70 eV and does not change significantly with water content. Measurements with different electrode configurations indicate its volume (bulk) character. These results suggest that peak IV may be the TSDC manifestation of the conductivity relaxation discussed in section DRS. The values of the activation energy of dc conductivity, reported below, strongly support this interpretation. Consistent with these experimental findings and by analogy to TSDC investigations of glass transitions in synthetic polymers [31, 33], the peak can also be related to the inhomogeneous character of samples (Maxwell-Wagner-Sillars interfacial polarization) and to the trapping of charges at the boundaries of different phases. Our experimental findings provide less support for attributing peak IV to a second glass transition associated with vibrational motions of the main chains of seed constituents [48, 49].

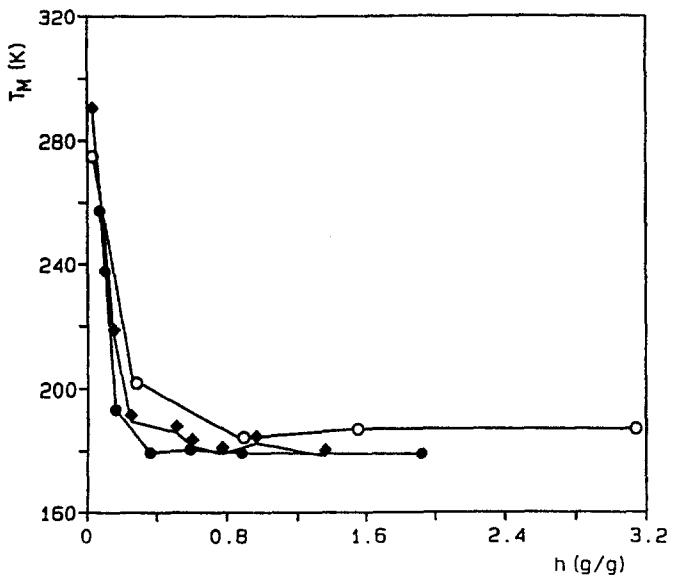

Fig. 11 Dependence of the peak temperature, T_M, of TSDC peak III, i.e. of T_g, on water content, h, for triticale (•), triticale endosperm (■), and triticale perisperm and pericarp (o)

Peak V is the dominant one in the HT band. Its properties were systematically studied within this work, and the following results were obtained. Its magnitude increases non-linearly with increasing polarizing field, E_p; it also depends on polarization temperature, T_p, and the electrode material. This peak increases in magnitude and shifts to lower temperatures with increasing water content. Its activation energy, determined from partial-heating experiments, is practically the same as that of peak III, peak IV, and dc conductivity. These findings suggest that peak V is associated with the release of space charges trapped at the sample-electrode interface. Electrochemical reactions are also likely to contribute to peak V.

All samples exhibit an apparent dc conductivity that begins in the temperature range of peak III. The dc current increases sharply with temperature (Fig. 7), especially at high h values. The temperature dependence of dc conductivity is Arrhenius-type, with an activation energy, W, of about 1.0 eV at $h \leq 0.2$ and about 0.70 eV at higher water contents. At a given temperature, the dc conductivity increases strongly with increasing h, by about 4 orders of magnitude in the region of $h=0.15$–0.30 (Fig. 12). These results confirm the percolation character of charge transport, suggested from ac measurements [2, 15, 16]. At water contents lower than about 0.15, water molecules are isolated, and the dc conductivity is low. Above a percolation threshold (at $h \approx 0.15$–0.30), a connective path for long-range motion is established, so that protons can move from electrode to electrode, and dc conductivity increases sharply. The activation en-

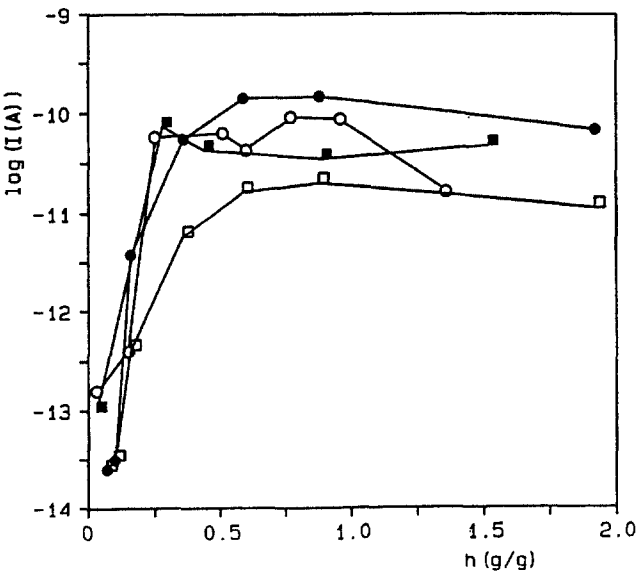

Fig. 12 Water-content dependence of dc conductivity current, measured for samples of triticale at 190 K (□) and 200 K (•), triticale endosperm at 200 K (o), and triticale perisperm and pericarp at 200 K (■)

ergy of dc conductivity (0.70 eV) is a little higher than the value proposed for the Grotthus proton transport mechanism (0.60 eV). The significance of percolative proton transfer to the emergence of biological functions has been extensively discussed in the literature [2, 15, 16].

Conclusions

In summary, the hydration properties of ground seeds of several cereals and legumes have been studied by means of DRS and three techniques of TSC (TSDC, TSPC, and thermally stimulated conductivity), over wide ranges of water contents and temperatures. The cereals, wheat and triticale, and the legumes, bean and horsebean, have been investigated in greatest detail. The main conclusions can be summarized as follows.

1) Several critical hydration levels have been identified by means of the different techniques used. TSDC and TSPC measurements have revealed that water molecules, corresponding to levels up to $h=0.11$ in wheat and $h=0.17$ in bean, are irrotationally bound at primary hydration sites, whereas at higher water contents, water molecules start to form clusters. It followed from DRS ac conductivity measurements that the seed/water system is homogeneous at $h<0.30$ but heterogeneous at $h>0.30$, in the sense that a separate water phase exists for $h>0.30$. These measurements allowed us to follow the freezing and melting of water in heterogeneous systems. Finally, TSC measurements showed that the seeds are fully hydrated [5] at $h\geq0.50$, in the sense that water in excess of $h\approx0.50$ exhibits bulk-water behaviour.

2) TSC measurements provided a good measure of T_g of the seeds. T_g is around room temperature for dry seeds and shifts down to about 180 K for fully hydrated seeds. The dependence of T_g on h is practically the same for powders from different parts of a seed (Fig. 11).

3) Dc conductivity and its activation energy were obtained, independently and in agreement, from presentation of DRS data in either the ac conductivity or modulus formalism and from TSC measurements. Dc conductivity increases sharply with increasing temperature at $T>T_g$, with an activation energy of about 0.60–0.70 eV for hydrated samples. Its dependence on water content suggests percolative transport of protons along threads of hydrogen-bonded water molecules, with a percolation threshold in the range of $h\approx0.15$–0.30. Note the proximity of the lower limit of this range to the fraction of water bound to primary hydration sites, and that of the upper limit to the critical hydration level separating homogeneous from heterogeneous systems.

4) With respect to the dependence of their physical properties on water content, cereals and legumes behave qualitatively the same. Furthermore, some quantitative results were practically the same, such as the critical level separat-

ing homogeneous from heterogeneous systems ($h \approx 0.30$). Other h values were different, the difference being attributed to the higher ratio of proteins/carbohydrates in legumes than in cereals and to the different hydration properties of proteins and carbohydrates. The water fraction corresponding to irrotationally (tightly) bound water molecules at primary hydration sites was 0.11 in wheat and 0.17 in bean. The ac conductivity at $h \leq 0.30$ was (at low frequencies) higher, by 1–2 orders of magnitude. In addition, the frequency dependence of ac conductivity suggests that bean is more conductor-like than is wheat.

5) DRS measurements suggested that frequency scans in the kHz–MHz range could provide a basis for non-destructive measurements of water content in seed powders.

* * *

Financial support through the Greek Ministry of Industry, Energy and Technology (Secretariat of Research and Technology), the Czech Ministry of Education, Youth and Sport (Dept. of International Scientific and Technological Cooperation), and the Empirikos Foundation is gratefully acknowledged.

References

1 C. Mok and J. W. Dick, Cereal Chem., 68 (1991) 405.
2 F. Bruni, in Correlations and Connectivity: Geometric Aspects of Physics, Chemistry and Biology, H. E. Stanley and N. Ostrowsky (eds.), Kluwer, Dordrecht 1990, p. 266.
3 S. Ratkovic and M. Denic, Genetica, 20 (1988) 113.
4 R. J. Williams and A.C. Leopold, Plant Physiol., 89 (1989) 977.
5 C.W.Vertucci, Biophys. J., 58 (1990) 1463.
6 C. F. Jenner and G. P. Jones, Austr. J. Plant Physiol., 17 (1990) 107.
7 S. Ratkovic and P. Pissis, J. Mater. Sci., in press.
8 S. S. Singh, M. F. Finner, P. K. Pohatgi, F. H. Buelow and M. Schaller, J. Mater. Sci., 26 (1991) 274.
9 M. Peleg, Rheol. Acta, 32 (1993) 575.
10 M. Peleg, Biotechnol. Prog., 10 (1994) 385.
11 N. L. Nolan, J. M. Faubion and R. C. Hoseney, Cereal Chem., 63 (1986) 287.
12 F. Bruni, in Correlations and Connectivity: Geometric Aspects of Physics, Chemistry and Biology, H. E. Stanley and N. Ostrowsky (eds.), Kluwer, Dordrecht 1990, p. 272.
13 F. Bruni and A. C. Leopold, Plant Physiol., 96 (1991) 660.
14 F. Bruni and A. C. Leopold, Biophys. J., 63 (1992) 663.
15 G. Carreri and A. Giansanti, Lett. Nuovo Cimento, 40 (1984) 193.
16 F. Bruni, G. Carreri and A. C. Leopold, Phys. Rev. A, 40 (1989) 2803.
17 T. Y. Shegoleva, Biofizika, 29 (1984) 690.
18 F. L. Shafer, D. Smith and J. A. Roberts, J. Microwave Power, 21 (1986) 167.
19 M. G. Holmes, K. McCallum and A. D. Diament, Seed Sci. Technol., 19 (1991) 413.
20 A.W. Kraszewski, T.-S. You and S. O. Nelson, IEEE Trans. Instrum. Meas., 38 (1989) 79.
21 A. Kraszewski and S. O. Nelson, J. Agric. Eng. Res., 43 (1989) 211.
22 S. O. Nelson, IEEE Trans. Electr. Insul., 26 (1991) 845.
23 A. W. Kraszewski and S. O. Nelson, Can. Agric. Eng., 34 (1992) 327.
24 S. O. Nelson, J. Food Eng., 21 (1994) 365.
25 I. D. Kuntz and W. Kauzmann, Adv. Prot. Chem., 28 (1974) 239.
26 J. A. Rupley and G. Careri, Adv. Prot. Chem., 41 (1991) 37.

27 H. Levine and L. Slade, in Physical Chemistry of Foods, H. G. Schwartzberg and R. W. Hartel (eds.), Marcel Dekker, NY 1992, p. 83.
28 R.B. Gregory, in Protein-Solvent Interactions, R. B. Gregory (ed.), Marcel Dekker, NY 1995, p. 191.
29 J. L. Finney and P. L. Poole, Comm. Mol. Cell. Biophys., 2 (1984) 129.
30 M. Tabellout, P.-Y. Baillif, H. Randrianantoandro, F. Litzinger, J. R. Emery, T. Nicolai and D. Durand, Phys. Rev. B, 51 (1995) 12295.
31 P. Pissis and L. Apekis, J. Non-Cryst. Solids, 131–3 (1991) 95.
32 A. Kyritsis, P. Pissis, J. L. Gomez Ribelles and M. Monleon Pradas, J. Non-Cryst. Solids, 172–4 (1994) 1041.
33 A. Kyritsis, P. Pissis, J. L. Gomez Ribelles and M. Monleon Pradas, J. Polym. Sci.: Polym. Phys. Ed., 32 (1994) 1001.
34 J. Mijovic, J. M. Kenny, A. Maffezzoli, A. Trivisano, F. Bellucci and L. Nicolais, Compos. Sci. Technol., 49 (1993) 277.
35 A. Kyritsis, P. Pissis and J. Grammatikakis, J. Polym. Sci: Polym. Phys. Ed., 33 (1995) 1737.
36 P. Braunlich (ed.), Thermally Stimulated Relaxations in Solids, Springer, Berlin 1979.
37 J. van Turnhout, in Topics in Applied Physics, Volume 33: Electrets, G. M. Sessler (ed.), Springer, Berlin 1980, p. 81.
38 J. Laudat and F. Laudat, Chem. Listy, 85 (1991) 941.
39 P. Pissis, A. Anagnostopoulou-Konsta, L. Apekis, D. Daoukaki-Diamanti and C. Christodoulides, J. Non-Cryst. Solids, 131–133 (1991) 1174.
40 R. Pethig, Dielectric and Electronic Properties of Biological Materials, Wiley, Chichester 1979.
41 P. Hedvig, Dielectric Spectroscopy of Polymers, Hilger, Bristol 1977.
42 J. R. MacDonald (ed.), Impedance Spectroscopy, Wiley, New York 1987.
43 P. B. Macedo, C. D. Moynihan and R. Bose, Phys. Chem. Glasses, 13 (1972) 171.
44 H.W. Starkweather, in Water in Polymers, S. P. Rowland (ed.), ACS Symposium Series 127, American Chemical Society, Washington, DC 1980, p. 433.
45 A. Anagnostopoulou-Konsta and P. Pissis, J. Phys. D: Appl. Phys., 20 (1987) 1168.
46 P. Pissis and A. Anagnostopoulou-Konsta, in Proceed. 5th Int. Symp. Electrets, G. M. Sessler and R. Gerhard-Mulhaupt (eds.), IEEE, New York 1985, p. 842.
47 J. Laudat and F. Laudat, Europhys. Lett., 20 (1992) 663.
48 P. Pissis, A. Anagnostopoulou-Konsta, L. Apekis, D. Daoukaki, C. Christodoulides and E. G. Sideris, IEEE Trans. El. Ins., 27 (1992) 820.
49 G. Carreri, G. Consolini and F. Bruni, Biophys. Chem., 37 (1990) 165.